

LA-UR-18-26923 (Accepted Manuscript)

Increased Mortality in Mice following Immunoprophylaxis Therapy with High Dosage of Nicotinamide in Persistent Infections

Micheva-Viteva, Sofiya N.
Ross, Brittany
Gao, Jun
Adikari, Samantha Hiroshini
Zhang, Pengfei
Mourant, Judith R.
Werner, James Henry
Torres, Alfredo
Hong-Geller, Elizabeth

Provided by the author(s) and the Los Alamos National Laboratory (2019-04-01).

To be published in: Infection and Immunity

DOI to publisher's version: 10.1128/IAI.00592-18

Permalink to record: <http://permalink.lanl.gov/object/view?what=info:lanl-repo/lareport/LA-UR-18-26923>

Disclaimer:

Los Alamos National Laboratory, an affirmative action/equal opportunity employer, is operated by Triad National Security, LLC for the National Nuclear Security Administration of U.S. Department of Energy under contract 89233218CNA000001. By approving this article, the publisher recognizes that the U.S. Government retains nonexclusive, royalty-free license to publish or reproduce the published form of this contribution, or to allow others to do so, for U.S. Government purposes. Los Alamos National Laboratory requests that the publisher identify this article as work performed under the auspices of the U.S. Department of Energy. Los Alamos National Laboratory strongly supports academic freedom and a researcher's right to publish; as an institution, however, the Laboratory does not endorse the viewpoint of a publication or guarantee its technical correctness.

1 **Increased mortality in mice following immunoprophylaxis therapy with high**
2 **dosage of nicotinamide in *Burkholderia* persistent infections**

3

4 Sofiya N. Micheva-Viteva^a, Brittany N. Ross^b, Jun Gao^a, Samantha Adikari^a, Pengfei Zhang^c,
5 Judith R. Mourant^a, Terry H. Wu^d, James H. Werner^c, Alfredo G. Torres^b, , and Elizabeth Hong-
6 Geller^{a,#}

7

8 ^aBioscience Division, Los Alamos National Laboratory, Los Alamos, NM 87545

9 ^bDepartment of Microbiology and Immunology, University of Texas Medical Branch, Galveston,
10 TX, 77555

11 ^cCenter for Integrated Nanotechnologies, Los Alamos National Laboratory, Los Alamos, 87545

12 ^dUniversity of New Mexico Health Sciences Center, Department of Internal Medicine,
13 Albuquerque, NM

14

15

16 [#]Corresponding Author

17 505-665-2465

18 ehong@lanl.gov

19

20 Running Title: Effect of nicotinamide on *Burkholderia* infection

21 **Abstract**

22 Bacterial persistence, known as non-inherited antibacterial resistance, is a contributing factor to
23 the establishment of long-lasting chronic bacterial infections. In this study, we examined the
24 ability of nicotinamide (NA) to potentiate different classes of antibiotics against *Burkholderia*
25 *thailandensis* persister cells. Here we demonstrate that addition of NA in *in vitro* models of *B.*
26 *thailandensis* infection resulted in a significant depletion of the persister population in response
27 to various classes of antibiotics. We applied microfluidic bioreactors with a continuous media
28 flow to study the effect of supplementation with a NA gradient on the recovery of *B.*
29 *thailandensis* persister populations. A co-culture of human neutrophils pre-activated with 50 μ M
30 NA and *B. thailandensis* resulted in the most efficient reduction in the persister population.
31 Applying single cell RNA FISH analysis and quantitative PCR, we found that NA inhibited gene
32 expression of the stringent response regulator *relA*, implicated in the regulation of the persister
33 metabolic state. We also demonstrate that a therapeutic dose of NA (250mg/kg), previously
34 applied as immunoprophylaxis against antibiotic-resistant bacterial species, produced adverse
35 effects in an *in vivo* murine infection model of the highly pathogenic *Burkholderia pseudomallei*,
36 indicating that therapeutic dose and metabolite effects have to be carefully evaluated and tailored
37 for every case of potential clinical application.

38

39 Introduction

40 There is an urgent need to develop novel antimicrobial therapies to combat the rapid spread of
41 antibiotic-resistant bacteria. In addition to the well-studied evolution of genetic resistance to
42 antibiotics, bacteria can also enter a dormant metabolic state, termed bacterial persistence or non-
43 inherited antibacterial resistance, in which cells undergo phenotypic changes that render them
44 refractory to virtually all known classes of antibiotics, thus leading to recurrence of chronic
45 infections and biofilm formation. [1-3] Bacterial persistence has been described more recently as
46 an evolutionarily-conserved mechanism that serves as community life insurance against a hostile
47 environment. [4] Multiple redundant pathways are thought to contribute to the establishment of
48 the persister metabolic state, including accumulation of the stringent response signaling
49 nucleotide (p)ppGpp, activity of the Lon protease, and toxin/antitoxin modules. [5, 6] In
50 addition, messenger RNA endonucleases, including RelE, MazF, and YafQ, and phosphorylation
51 of glutamyl-transfer RNA synthetase GltX have been attributed to the establishment of
52 persistence. [7, 8] Given the multiple mechanisms that regulate persistence, therapeutic
53 development to eradicate persister cells remains particularly challenging.

54 Several promising strategies that target bacterial persistence have been reported. Since persisters
55 are thought to have reduced metabolic activity, stimulation of metabolic pathways may reactivate
56 persister growth, thus making them more susceptible to antibiotic treatment. In support of this
57 hypothesis, addition of metabolites that fuel glycolysis, such as glucose, mannitol, and fructose,
58 have led to an increase in aminoglycoside antibiotic uptake through stimulation of the proton
59 motive force and subsequent enhanced killing of persisters in *E. coli*. [9] Persisters have also
60 been depleted by supplementation of conventional antibiotics with novel antibacterial classes,
61 such as acyldepsipeptides (ADEPs). [9, 10] ADEPs deregulate ClpP protease activity, leading to

62 uncontrolled protease degradation, inhibition of cell division, and eventually cell death. [11, 12]
63 However, ADEPs have very limited activity against Gram-negative bacteria. *clpP* mutants
64 resistant to ADEP arise with high frequency because ClpP is not essential for the bacterial
65 lifecycle. [11]

66 To further investigate metabolite-mediated strategies to target bacterial persistence, we examined
67 the ability of nicotinamide (NA) to potentiate different classes of antibiotics against persisters in
68 *Burkholderia thailandensis* CDC2721122, a clinical isolate from a pleural wound. NA, also
69 known as vitamin B3, is a precursor of nicotinamide adenosine dinucleotide (NAD), a key co-
70 factor for enzymes that play a role in oxidative phosphorylation. We hypothesized that NA
71 could potentially kickstart energy metabolism to a level sufficient for bacteria to exit the
72 persistence state and thus recover sensitivity to antibiotics. In addition, NA has been shown to
73 stimulate killing of *S. aureus* and *C. rodentium* in murine models [13, 14]. We demonstrated a
74 significant depletion of the persister population in response to various classes of antibiotics when
75 we applied NA in *in vitro* models of *B. thailandensis* infection. However, the use of NA in an *in*
76 *vivo* murine infection model of *Burkholderia pseudomallei*, a highly pathogenic Select Agent
77 that is closely related to *B. thailandensis* and causes the infectious disease melioidosis, produced
78 unexpected adverse effects, indicating that NA will likely not be therapeutically effective when
79 supplied at a high dose. Here, we raise awareness that therapeutic strategies previously shown to
80 be successful in *in vivo* systems of opportunistic bacterial infections may be detrimental for
81 treatment of pathogens that target innate immune responses.

82

83 Results

84 *NA potentiated the bactericidal effect of various antibiotics against B. thailandensis persisters*

85 We observed that the size of the persister population within planktonic *B. thailandensis*
86 CDC2721122 cultures varied depending on the class of antibiotic used. Ofloxacin (Oflx), a
87 fluoroquinolone that targets DNA replication, was 50-fold and 100-fold more effective in killing
88 persisters, compared to ceftazidime (Ceftz) and trimethoprim (Tmp), respectively (Fig. 1A). We
89 also noted that *Burkholderia* cells entered persistence at a higher rate than previously-studied
90 organisms, up to 1% in stationary phase compared to 0.1% in *E. coli* (Fig. 1A-B) [15-17].
91 Consistent with the bacterial stringent response to nutrient limitation, the size of *B. thailandensis*
92 persister populations was ~10-fold higher in stationary phase compared to exponentially dividing
93 cells (Fig. 1A-B). Addition of 1 mM NA prior to antibiotic treatment decreased persisters by
94 >10-fold in both exponential and stationary phase *B. thailandensis* cultures treated with each of
95 the three antibiotics, indicating that NA can potentiate the antibiotic-mediated killing of
96 persisters (Fig. 1A).

97 Ceftz, a β -lactam antibiotic, has been an effective therapy for melioidosis, the infectious disease
98 associated with *B. pseudomallei* infection. Two regimens are commonly prescribed for initial
99 treatment of severe melioidosis: (1) Ceftz monotherapy and (2) Ceftz in combination with
100 trimethoprim-sulfamethoxazole (Tmp-SMX) [18]. While the combination therapy has not been
101 reported to have an advantage over the monotherapy in cases of acute melioidosis, it is possible
102 that the Tmp-SMX component could potentiate the Ceftz treatment by reducing *Burkholderia*
103 persisters. To test this *in vitro*, we treated *B. thailandensis* with Ceftz or a combination of Ceftz
104 and Tmp. Persisters were present at 0.1% and 0.3% at exponential phase and 1% and 2% at

105 stationary phase during Ceftz and Tmp monotherapy, respectively (Fig. 1A). Upon combination
106 treatment with Ceftz and Tmp, we registered >10-fold reduction in the percentage of persister
107 survival, compared to drug monotherapy, at the stationary phase (Fig. 1B). Addition of 1 mM
108 NA prior to the combination antibiotic therapy resulted in >10,000-fold depletion of persisters
109 compared to monotherapy with Tmp (Fig. 1B).

110 Given the role of NA as a precursor of the key metabolite NAD in the oxidative phosphorylation
111 pathway, we measured the total ATP pool in *B. thailandensis* treated with various concentrations
112 of NA. We detected a two-fold increase in the ATP pool in stationary phase cells treated with 1
113 mM NA, compared to cultures grown in the absence of NA. We did not see a similar increase
114 upon addition of 10 mM NA. NA did not boost ATP generation in exponentially dividing cells
115 (Fig.1C).

116 To further examine the effect of NA on antibiotic treatment of *B. thailandensis* persisters, we
117 simultaneously measured the ATP pool and cell density in *B. thailandensis* treated with 1x
118 minimal bactericidal concentration (1x MBC) of Oflox (100 µg/ml). In general, ATP content is
119 expected to linearly correlate with cellular density in exponentially dividing cells. Surprisingly,
120 we consistently registered a burst in ATP production in the first 3h of *B. thailandensis* treatment
121 with 1x MBC of Oflox, while cell density was observed to stay relatively flat. (Fig. 1 D-E, Oflox-
122 100 µg/ml). This effect was not observed when cells were treated with 2x MBC of Oflox (Fig. 1
123 D-E, Oflox-200 µg/ml), consistent with cell death at this bactericidal concentration and concurrent
124 with a decrease in cell density. Addition of 1 mM NA to bacterial cultures treated with 1x MBC
125 Oflox resulted in a two-fold reduction of ATP levels compared to treatment with 1x MBC alone,
126 although the ATP pool remained 2.5-fold higher than the untreated, exponentially dividing cells
127 (Fig. 1D, Oflox-100+NA). The observed ATP burst and decrease with NA supplementation was

128 also observed in cells treated with 1x MBC levels of meropenem (Mpm), indicating that the
129 observed effect is independent of the antibiotic mechanism of action (Fig. S1). These results
130 suggest that suboptimal bactericidal antibiotic concentrations can stimulate the ATP production
131 that may be needed to fuel metabolic pathways that can induce onset of persistence. Addition of
132 NA resulted in partial rescue of the enhanced ATP production, which may contribute to
133 reduction in persistence. Thus far, the data indicate that a combination of NA with different
134 classes of antibiotics may be a viable approach for more effective treatment of pathogen
135 infection.

136

137 ***NA can increase susceptibility of *B. thailandensis* persister cells to antibiotics***

138 We utilized a microfluidics platform to simulate the microscale environment and fluid dynamics
139 of the host circulatory system, as would be observed during bacteremia, to determine the NA
140 concentration at which *Burkholderia* persister populations become most sensitive to the
141 antibiotic bactericidal effect (Fig. S2A). We generated NA concentration gradients from 0 to
142 100 μM by applying a microfluidic picoliter bioreactor as previously described [19]. We
143 observed that NA had little effect on bacterial growth at low concentrations (Fig. 2A, top half),
144 but started to exhibit a bacteriostatic effect at higher NA concentrations ($\sim 50\text{-}100\ \mu\text{M}$), in which
145 bacterial growth was inhibited (Fig. 2A, bottom half). Interestingly, this effect lasted for 24h
146 with continuous flow of media supplemented with NA, after which bacterial density became
147 more uniform throughout the microfluidic channels, suggesting that *Burkholderia* are capable of
148 overcoming the NA-mediated bacteriostatic effect (Data not shown).

149 We also applied microfluidic devices containing cell trapper chambers that can corral bacteria
150 into a partially enclosed area for concentrated bacterial growth during fluid flow. We observed
151 inhibition of bacterial growth in these trappers at estimated NA concentration $\sim 50 \mu\text{M}$ (Fig. 2B,
152 bottom trappers). We further studied the dosage effect of NA on *Burkholderia* sensitivity to
153 antibiotics. *B. thailandensis* was pre-incubated in a NA concentration gradient for 24h, exposed
154 to either Mpm (50 $\mu\text{g/ml}$) or Ceftz (50 $\mu\text{g/ml}$) for 48h, and then allowed to recover in NA- and
155 antibiotic-free LB for 4 days. We observed that cells receiving $\sim 4 \mu\text{M}$ NA prior to antibiotic
156 treatment exhibited low viability, as observed by high levels of propidium iodide (PI) staining of
157 dead cells in the growth chamber of the microfluidic bioreactor, suggesting that persisters were
158 susceptible to killing under these conditions (Fig. 2C, third panel from top). Pre-treatment of
159 cells with higher concentrations of NA ($>10 \mu\text{M}$) did not show the same effect. Metabolite
160 concentrations in the microfluidic bioreactor were estimated relative to the concentration
161 gradient of a colorimetric dye (Fig. S2B). We also confirmed the effects of 4, 16, and 25 μM NA
162 by applying a single concentration of the metabolite in the bioreactor (Fig. 2D and data not
163 shown). Taken together, our results indicate that there is a “sweet spot” of optimal NA
164 concentration at $\sim 4 \mu\text{M}$ that may switch persisters out of the dormant state and render them
165 responsive to killing by antibiotics. Importantly, the NA effective concentrations reflected the
166 scale of the bacterial growth environment: mM for milli-scale bacterial cultures (Fig. 1) and μM
167 for bacteria grown in the microfluidic channels (Fig. 2).

168

169 ***NA reduces *B. thailandensis* persisters by inhibition of the bacterial stringent response***
170 ***regulator RelA and stimulation of bactericidal effect in host neutrophils***

171 We investigated whether the NA-mediated decrease in *Burkholderia* persistence is linked to the
172 activity of RelA, which regulates the concentration of the ppGpp alarmone in response to various
173 environmental cues, including temperature change, nutrient limitations, and transition to
174 stationary phase. Cellular accumulation of ppGpp initiates stress responses referred to as the
175 "stringent response," which contributes to the establishment of the persister metabolic state [20,
176 21]. On average, the transcript levels of *relA* in stationary phase *B. thailandensis* cells ($\geq 1\%$
177 persisters) were >6-fold higher compared to cells grown at exponential phase ($\leq 0.1\%$ persisters),
178 as measured by qPCR. The *relA* transcript levels were reduced by ~3-fold in stationary phase
179 cells upon addition of NA in the culture media, indicating inhibition of the stringent response in
180 *B. thailandensis* by NA (Fig. 3A).

181 We further investigated the effect of NA on *relA* gene expression at the single cell level using
182 RNA-FISH (RNA-based fluorescence *in situ* hybridization). Consistent with the qPCR results,
183 *relA* gene expression was significantly higher in stationary phase *B. thailandensis* populations
184 compared to exponentially dividing bacterial populations (Fig. 3B). Addition of NA to *B.*
185 *thailandensis* cells at stationary phase inhibited *relA* expression compared to their untreated
186 counterparts. Interestingly, RNA-FISH analysis revealed a very small population ($\leq 0.01\%$) of *B.*
187 *thailandensis* cells in the exponential growth phase with *relA* fluorescence intensities comparable
188 to *relA* levels at stationary phase, suggesting that these outliers may be stochastically
189 overexpressing *relA* to cause a shift in these cells to persistence. Altogether, these results
190 suggest that NA can inhibit the stringent response and may reduce the population of persisters
191 that can survive antibiotic treatment.

192 To assess the therapeutic potential of NA in combination with antibiotic treatment, we employed
193 the microfluidic bioreactors described earlier to grow *B. thailandensis* cultures over several days

194 or weeks under continuous fluid flow and compared the time required for the re-population of
195 the growth chambers with bacteria surviving antibiotic treatment. Following 6 days of incubation
196 with 50 µg/ml Mpm in the microfluidic device, *B. thailandensis* monocultures contained mostly
197 dead cells, as determined by propidium iodine (PI) staining (data not shown). We next infused
198 the microfluidics device with antibiotic-free media to stimulate any persisters that remained
199 recalcitrant to Mpm and observed recovery of bacterial re-growth after 4 days of continuous
200 culture (Table 1). A combination of 4µM NA with Mpm treatment led to recovery of the *B.*
201 *thailandensis* persister population in 5 days, suggesting that NA reduced persister cell survival.
202 We also observed bacterial recovery after 4 days following incubation with 400 µg/ml Tmp, after
203 5 days with 50 mg/ml Oflox, and after 10 days with 100 µg/ml Oflox. We consistently observed an
204 increase in the number of days needed for *B. thailandensis* re-growth in the device when media
205 was supplemented with NA, regardless of the mechanism of antibiotic action (Table 1).

206 We further investigated *B. thailandensis* exposed to Mpm in the presence of human neutrophils,
207 to add a physiologically-relevant host immune function to the microfluidic bioreactor. Bacterial
208 co-culture with neutrophils at a 1:1 cell ratio resulted in a greater delay in bacterial re-growth
209 following Mpm treatment, occurring at 7 days post-antibiotic treatment. Addition of 25 µM NA
210 to *B. thailandensis*-neutrophil co-cultures treated with Mpm led to an even longer recovery time,
211 occurring at 12 days post-antibiotic treatment. Notably, a combination of Mpm with 4 µM NA
212 and neutrophil co-culture took 7 days for bacterial recovery, similar to co-culture in the absence
213 of NA. This observation suggested that higher NA doses may be required for stimulation of the
214 neutrophil bactericidal function. In support of this hypothesis, recovery of bacterial growth was
215 not observed till 15 days post-antibiotic treatment when neutrophils were pre-incubated with 50

216 μM NA for 24h prior to co-culture with *Burkholderia* and subsequent addition of 4 μM NA in
217 the growth media (Table 1).

218 We also examined whether the neutrophil-mediated bactericidal effect was in part due to NA-
219 stimulated release of neutrophil extracellular traps (NETs). NET formations consist of chromatin
220 enmeshed with granular and nuclear proteins and are known to capture and kill microbial cells
221 [22]. We infused the microfluidic devices with antibodies specific to human citrullinated histone
222 H3, a major protein component of the NETs [23], and detected antibody-labeled puncta (green
223 and yellow overlay stain) against the NET-like nucleic acid released formations (red stain) in
224 samples supplemented with NA, compared to bacteria-neutrophil co-cultures not treated with NA
225 (Fig. 4).

226

227 ***Immunoprophylaxis with NA exacerbated the outcome of infection in BALB/c mice exposed to***
228 ***B. pseudomallei K96243***

229 We performed *in vitro* studies with *Burkholderia pseudomallei* K96243 prior to testing the effect
230 of NA as a therapeutic supplement *in vivo*. NA was added to stationary phase cultures in
231 combination with 100xMIC levofloxacin treatment. The antibiotic potency against persisters was
232 examined 24h post treatment when the bactericidal effect reached a plateau [17]. We observed
233 no significant effect on the potency of levofloxacin against persisters at the lower concentrations
234 of 0.1 and 1 mM NA. However, a high dose of 10mM NA markedly increased the survival rate
235 of *B. pseudomallei* when combined with levofloxacin (Fig. 5A).

236 To determine whether NA could function as a therapeutic agent to augment antibiotic killing of
237 persisters and promote more effective immune-mediated killing, we applied NA as a
238 prophylactic agent prior to infection with *Burkholderia pseudomallei* K96243 in a murine model

239 of melioidosis. Both *B. thailandensis* and *B. pseudomallei* share significant genetic similarity and
240 resistance to various classes of antibiotics linked to efflux pump and β -lactamase activities [24,
241 25]. We based our treatment regimen on the previous successful use of NA on bacterial
242 infections in mice [13, 14] and on our *in vitro* data showing a stronger effect on persister
243 eradication when NA was introduced *prior* to antibiotic treatment. We administered 250 mg/kg
244 NA or PBS daily to BALB/c mice for 2 days and then exposed them to 2 LD₅₀ *B. pseudomallei*
245 via the intranasal route. Antibiotic treatment using levofloxacin alone or in combination with NA
246 was initiated 24h post-bacterial infection and lasted for 5 days. Two control groups, PBS or NA-
247 treated mice did not receive antibiotic.

248 Strikingly, the control group treated only with NA exhibited the most adverse response to *B.*
249 *pseudomallei* infection, showing irreversible weight loss and ruffled fur (severe clinical signs),
250 and 100% of the animals succumbed to infection within 7 days (Fig. 5B-C). Severe clinical signs
251 were also observed in half of the control animals receiving PBS. Greater than 50% of PBS
252 animals showed recovery past the 5th day of infection and survived up to 21 days post-infection
253 when the experiment was terminated. Consistent with the adverse effects of the NA treatment,
254 we recovered 10-fold and 10⁶-fold higher cfu of *B. pseudomallei* in the liver and the spleen,
255 respectively, for animals that received the NA/levofloxacin combination, compared to animals
256 that received only PBS (Fig. 5D-E). Bacterial counts in the lungs of animals treated with
257 NA/levofloxacin were similar to those of the PBS control group and were both 10-fold higher
258 than the counts of live bacteria from the lungs of animals treated with just levofloxacin (Fig. 5F).
259 Furthermore, at 21 days post-infection and prior to termination of the experiment, we observed
260 that the group treated with NA/levofloxacin started to show symptoms of infection resurgence,
261 which could be due to the very high bacteria counts in the spleen. Lobulated yellowish lesions

262 were observed only in the spleen of the animals treated with the combination of NA/levofloxacin
263 that survived till the end of the experiment (Fig. 5G). These formations are indicative of
264 granulomatous inflammation caused by activated epithelioid macrophages [26]. Altogether, our
265 *in vivo* results show that a high dose of NA led to an increase in *B. pseudomallei* spread and
266 colonization of target organs in a murine infection model.

267

268 **Discussion**

269 In addition to genetic inheritance of antibiotic resistance, many microbes also display bacterial
270 persistence or non-inherited antimicrobial resistance, in which a small percentage of the cell
271 population (0.01-0.1% in log growth *E. coli*) enter a near-dormant metabolic state and are
272 subsequently refractory to antibiotic killing. [15, 16] Metabolite-based strategies to kickstart
273 persisters into a metabolically-active state to potentiate antibiotic activity against persisters may
274 significantly improve the outcome of chronic bacterial infections. In this study, we found that
275 persistence occurs at comparatively higher frequencies in *B. thailandensis* (0.1-1% in log
276 growth), thus making *Burkholderia* an excellent bacterial species to further study persistence.

277 We observed that different antibiotics exhibited varied potency in killing persisters. For
278 example, Ofloxacin, which targets DNA gyrase, was more effective at killing persisters compared to
279 Trimethoprim or Ceftriaxone, which target dihydrofolate reductase and cell wall synthesis, respectively.
280 Although the potency of antibiotics against the persister population was varied, as evidenced by
281 the percentage of cell survival, the phenomenon of persistence was universal since no antibiotic
282 alone was capable of completely eradicating the persister population. The varied survival rates of
283 persisters in response to antibiotics with different mechanisms of action indicate that there are
284 different pathways to establish persistence. Interestingly, exposure to a minimum bactericidal
285 dose of antibiotics led to a boost in ATP accumulation in the first three hours, suggesting that
286 antibiotics can initially stimulate energy generation. Antibiotic treatment has been reported to
287 stimulate energy-consuming secondary metabolic pathways and activation of efflux pumps,
288 establishing a link between bactericidal lethality and antibiotic-induced cellular respiration. [27,
289 28] Bacteriostatic antibiotic treatment of *E. coli* and *S. aureus* has been shown to lead to
290 accumulation of energy metabolites that feed the electron transport chain. [27] Thus, we

291 speculate that the tipping point for whether a bacterial cell dies or becomes persistent in response
292 to antibiotics is dependent on the stimulated level of energy generation in each individual cell.

293 We also demonstrate that the metabolite NA could potentiate the bactericidal effect of different
294 antibiotics against *B. thailandensis in vitro*. NA is a precursor of NAD, a co-enzyme in the
295 glycolysis and the Krebs cycle metabolic pathways. NAD is transformed into NADH by
296 accepting electrons in several reactions involved in energy metabolism. For each pair of
297 electrons passed along the electron transport chain, one NADH is used and three ATP molecules
298 are generated. NA was also shown to inhibit poly-ADP-ribose polymerase, which is responsible
299 for NAD depletion by transferring poly-ADP-ribose subunits from NAD to various DNA repair
300 enzymes. [29] Our finding that NA also inhibited the transcription of *relA* in *B. thailandensis*
301 during stationary phase is consistent with NA acting to stimulate persister growth. RelA is a key
302 regulator of the stringent response during times of stressful environmental conditions, allowing
303 bacteria to rapidly divert energy and resources towards processes that ensure cell survival. [30-
304 32]

305 In previous studies, NA had been shown to significantly relieve disease symptoms in mouse
306 models of Parkinson's and Huntington's diseases [33, 34]. NA has been used as an
307 immunomodulation agent to suppress secretion of pro-inflammatory cytokines and chemokines
308 [35-37], and to improve host survival during murine models of sepsis [36, 38]. Furthermore, NA
309 has been tested as an antimicrobial therapeutic agent in murine models of infection caused by
310 opportunistic pathogens, including *Staphylococcus aureus* and *Citrobacter rodentium*, and was
311 found to stimulate host neutrophil cells to release microbicidal peptides by direct activation of
312 myeloid-specific transcription factor CCAAT/enhancer-binding protein ϵ (C/EBP ϵ) [13, 14].
313 Because NA was found to have a therapeutic effect in previous infection models, we utilized two

314 systems to assess NA-assisted antibiotic killing of *Burkholderia*: (1) microfluidic devices under
315 continuous flow of nutrient media to simulate the host circulatory system, and (2) *in vivo* murine
316 model of *B. pseudomallei* infection. The microfluidic devices allowed us to generate
317 concentration gradients of NA to assess the *B. thailandensis* response to antibiotic treatment in a
318 single device. We observed that while high doses of NA (~100 μ M) have a bacteriostatic effect
319 and may contribute to the increase in the percentage of persister cells, lower NA levels (<25 μ M)
320 combined with human neutrophils, was the most efficacious regimen tested for elimination of *B.*
321 *thailandensis* persisters. We also observed that human neutrophils pre-treated with NA
322 efficiently released a meshwork of chromatin fibers, structures known as neutrophil extracellular
323 traps (NETs), when in co-culture with *B. thailandensis*. In addition to the chromatin fibers, NETs
324 consist of antimicrobial peptides and enzymes and are considered an important strategy to trap
325 and kill microorganisms [39-41].

326 Our initial success using NA to eliminate persisters in the microfluidic devices led us to test NA
327 as a prophylactic treatment using an *in vivo* murine model of *B. pseudomallei* infection.
328 Although NA at low concentrations (0.1 and 1mM) did not induce a significant change in *B.*
329 *pseudomallei* persister survival to levofloxacin when added to stationary phase cultures *in vitro*,
330 a high 10 mM NA concentration led to increased *B. pseudomallei* persister survival. To test
331 these results in *in vivo* studies, we applied the therapeutic concentration of NA, 250 mg/kg,
332 previously used for *in vivo* animal studies of bacterial infection. For comparison, the maximum
333 daily tolerated dose of NA in humans is 6 g, with an average maximum recorded plasma level
334 (mean \pm 1 SEM) of 156.4 \pm 33.6 μ g/ml [42], which is about half the dose in the murine
335 studies. While NA had stimulated immune-mediated killing of *S. aureus* and *C. rodentium* in
336 murine models [13, 14], we observed an extremely adverse effect in response to infection of

337 BALB/c mice with 2 LD₅₀ *B. pseudomallei* K96243 receiving 250 mg/kg/d NA administered
338 alone. There was 100% mortality in the animal group that received NA as a prophylactic with no
339 antibiotic supplementation, compared to 50% mortality in the group treated solely with saline
340 solution. Given that NA has been reported to enhance neutrophil killing of bacteria in mice [13]
341 and increase the number of neutrophils in peripheral blood of humans [43], we hypothesize that
342 NA may hyper-stimulate the host immune response, specifically the neutrophil function, leading
343 to rapid animal death upon *B. pseudomallei* infection. Interestingly, adverse immune responses
344 were not reported when 250 mg/kg/d NA was used in the *S. aureus* and *C. rodentium* mouse
345 infection studies.

346 It is likely that the NA concentration is a key determinant whose potentiation effect will vary
347 depending on the metabolism of the specific bacterial species. Our studies suggest that the NA
348 effect as an auxiliary metabolite to the antibiotic activity against persister populations may be a
349 general phenomenon in some species. We have also observed that NA is capable of potentiating
350 antibiotic activity against *Pseudomonas aeruginosa* under similar experimental conditions to that
351 of our *B. thailandensis* studies. (Data not shown) Although we found that a high dose of NA was
352 detrimental for animals during infection with *B. pseudomallei*, it may be the case that lower
353 doses of NA (e.g. 5-10 mg/kg/d) continuously administered using an optimized route following
354 infection could improve antibiotic efficiency against persister cells. It was previously shown that
355 40 μ M NA could inhibit IL-1 β , IL-6 and TNF α cytokine responses by >95% in *in vitro*
356 stimulated human whole blood cells by endotoxin [35]. Inhibition of systemic inflammatory
357 responses have the potential to increase the survival outcome from lethal *B. pseudomallei*
358 infections. For example, immunomodulation via the COX-2 inhibitor significantly improved
359 antimicrobial treatment efficacy in BALB/c mice after lethal pulmonary infection with *B.*

360 *pseudomallei*, resulting in a lower bacterial burden in the spleen. [44] Testing lower doses of NA
361 or alternative routes of administration as a prophylactic treatment of *Burkholderia* infection
362 could be the focus of future studies.

363

364 Due to the rise of antibiotic resistance amongst pathogenic bacteria, there is growing interest
365 towards developing therapeutic approaches based on the modulation of the host immune
366 response. The results from our study caution us to carefully evaluate each therapeutic approach
367 involving immunomodulation and to tailor it to the specificities of the immune response to each
368 pathogen, since there is great variance in the outcome of host-pathogen interactions.

369

370 **Materials and Methods**

371

372 **Bacterial Strains.** *B. thailandensis* CDC2721121 cultures were grown in LB medium overnight
373 at 37°C. Antibiotic sensitivity tests were performed in LB medium at 37°C with aeration or in
374 microfluidic bioreactors with continuous flow of LB medium. *B. pseudomallei* K96243 (BEI
375 Resources, Manassas, VA, USA) was used in the murine infection experiment. *B. pseudomallei*
376 was propagated on LB agar and then LB medium at 37°C. All manipulations of *B. pseudomallei*
377 were conducted in compliance with the Select Agent regulations and in a CDC/USDA-approved
378 and registered biosafety level 3 (BSL3) facilities at the University of Texas Medical Branch
379 (UTMB).

380 **Human tissue culture.** Normal human neutrophils (NHN) were obtained from Astarte Biologics
381 (Bothell, WA, Cat#1025), and cultured in RPMI media (Invitrogen, Carlsbad, CA) supplemented
382 with 5% fetal bovine serum and 2 mM L-glutamine in a 5% CO₂ humidified incubator at 37°C
383 for 24h prior to experimental manipulations. For 24h pretreatment of human neutrophils, NA
384 was added immediately after thawing of the cells, since we observed clumping of NHN cells and
385 decreased viability after 40h of incubation, as measured by Trypan blue staining.

386 **Determination of Minimum Inhibitory Concentration (MIC) and bacterial persistence**
387 **fraction.** MICs for antibiotics were determined in LB medium by microdilution following
388 standard NCCLS protocols. The MICs were determined as the antibiotic concentration at which
389 the OD₆₀₀ remained unchanged within 24h of bacterial culture, compared to the seeding density.
390 Ceftz (#C0690500), Mpm (# 392454), Tpm (#T7883), and Oflox (#1478108) were obtained from
391 Sigma-Aldrich (St. Louis, MO). To determine the population of persister cells we inoculated 2ml
392 Luria Broth (Miller, Fisher Scientific) in 5ml Falcon tubes with one colony of *B. thailandensis*

393 from a LB agar plate and bacteria were incubated at 37°C with low aeration at 120 rpm until the
394 optical density reached 0.2 OD₆₀₀ prior to addition of antibiotics for the exponential growth
395 samples. To test the effect of NA on the antibiotic-mediated bactericidal effect, the metabolite
396 was supplemented in the culture media prior to addition of antibiotics. Limiting dilutions of
397 bacterial cultures prior to addition of antibiotic were plated on antibiotic free LB agar plates to
398 determine the bacterial counts at 0h time point as colony forming units, CFU/ml. Stationary
399 phase samples originated from overnight bacterial cultures incubated in media supplemented
400 with NA without aeration, and media with antibiotic was added at 1:1 dilution ratio. Percentage
401 survival of persisters was determined after 24h of antibiotic treatment. *In vitro* experiments with
402 *B. pseudomallei* cultures were performed without NA supplementation prior to antibiotic
403 treatment. Stationary *B. pseudomallei* were adjusted to 1×10^8 cfu per well and treated with 100x
404 MIC (400µl) of levofloxacin or ceftazidime in combination with NA at a final concentration of
405 0, 0.1, 1, or 10mM. At 24 hours post-antibiotic treatment, bacteria were collected, resuspended in
406 fresh media, and plated for cfu enumeration. The number of surviving bacteria was normalized
407 by the input and displayed as percent survival. CFUs, per ml culture, were determined by plating
408 serial dilutions of bacterial cells on antibiotic-free LB agar plates and counting colonies after 24-
409 48h incubation at 37°C. The percentage survival of drug tolerant persister cells was determined
410 by exposing bacterial cultures to antibiotics at 200x the MIC for Ceftz and Tpm and 100x the
411 MIC for Mpm and Oflox. After antibiotic treatment, bacterial cultures were pelleted and
412 resuspended in 1ml antibiotic-free LB medium. Percentage survival was determined as viable
413 CFU counts following 10-fold serial dilution in LB medium and plating on LB agar as a fraction
414 of the CFU count of input culture. All assays were performed in triplicate. Tests for genetically-

415 acquired antibiotic resistance was performed by plating bacterial cultures surviving antibiotic
416 treatment on LB agar plates containing antibiotic under 50×MIC.

417 **ATP pool determination.** We applied the Bac Titer-Glo Microbial Cell Viability assay
418 (Promega) to measure the ATP content in bacterial samples immediately after obtaining OD₆₀₀
419 values at particular time points of bacterial culture growth and/or antibiotic treatment. The assay
420 was performed in 96-well format, adding 1:1 ratio of Bac Titer-Glo Reagent to bacterial samples
421 (100 µL). Triplicate measurements of relative light units, RLU, per sample were performed and
422 average values calculated.

423 **Isolation of bacterial RNA and quantitative RT-PCR.** Total RNA was isolated from bacterial
424 pellets pre-incubated in 1000 U lysozyme for 15 min at 37°C and dissolved in TRIzol reagent
425 (1ml reagent per 10⁸ bacteria). Chloroform was added to the TRIzol extract (1:4 ratio) and
426 samples were incubated at room temperature for 5 min. The aqueous phase containing RNA was
427 separated from the organic phase by centrifugation for 15 min at 12,000g (8°C). An equal
428 volume of 100% chilled ethanol was added to the RNA solution and then loaded on a RNA-
429 binding column from the miRNeasy Kit (QIAGEN). RNA was eluted in water, and residual
430 genomic DNA was removed by treatment with the TURBO DNA-free Kit (Thermo Fisher
431 Scientific). The RNA concentration was determined using the ND1000 Nano-drop
432 spectrophotometer (Thermo Scientific), and RNA quality was evaluated on a denaturing 1%
433 agarose gel. The Power SYBR Green RNA-to-Ct 1-Step Kit (Thermo Fisher Scientific for
434 Applied Biosystems) was used to perform RT-PCR for transcript calculations. For each RT-PCR
435 reaction, transcript-specific forward and reverse primers (final concentration 600 pmol) were
436 used: RelA_fw 5'AAT TCC TCG AGC ACG TGA AG; RelA_rev 5'GAG ATC GCT GTG GAT
437 CGA ATA C; dnaJ_fw 5'CAG GGC TTC TTC AGC ATT CA; dnaJ_rev 5'GTG AAG GAA

438 ACC AAG ACG CT; 16S/rrsD_fw 5'AGG CCT TCG GGT TGT AAA G; 16S/rrsD_rev 5'GTA
439 GTT AGC CGG TGC TTA TTC T. The RT-PCR reactions were performed on the ABI7500 Fast
440 System (Applied Biosystems) with cycling conditions according to the manufacturer's protocol
441 for the Power SYBR Green RNA-to-Ct 1-step Kit. *relA* gene transcript levels were normalized to
442 the 16S rRNA. *dnaJ* transcripts were used as a second normalization control since their
443 abundance was comparable to *relA* expression and remained unchanged in all test conditions.
444 RNA ratios were calculated relative to the control sample, *B. thailandensis* growing cultures with
445 no treatment, by applying the $\Delta\Delta\text{CT}$ method. RT-PCR products for each transcript were
446 validated via sequencing.

447 **RNA FISH experiments for single cell analysis.** A RNA hybridization probe set for *relA* mRNA
448 consisting of 40 Quasar 560 labeled antisense oligonucleotides was purchased from Biosearch
449 Technologies utilizing the company's probe designer tool. The probe set was diluted to 100 μM
450 in nuclease-free water and aliquoted in 5 μL batches for subsequent experiments. Bacterial pellets
451 from exponentially-dividing cells ($\text{OD}_{600} \sim 0.4$) and stationary growth phase cultures (OD_{600}
452 ~ 1.2) were collected by centrifugation at 6000g for 5 min and fixed in 3.7% formaldehyde for 60
453 min at room temperature, followed by overnight permeabilization in 70% ethanol at 4°C. Fixed
454 and permeabilized bacterial samples were washed once with 2 \times saline sodium citrate (SSC)
455 buffer containing 2% deionized formamide and resuspended in 100 μL of hybridization buffer
456 (1g dextran sulfate, 10 mg *E.coli* tRNA, 100 μL of 200 mM vanadyl ribonucleoside complex, 40
457 μL of 5 mg/mL BSA, 1 mL 20 \times SSC, 2 mL deionized formamide) with a final volume of 10 mL.
458 The probe set was diluted in hybridization buffer at a 1:100 ratio to final concentration 1 μM .
459 Samples were incubated overnight at 30°C in the dark. The bacteria were then pelleted by
460 centrifugation and washed twice with 500 μL of 2 \times SSC buffer containing 2% formamide and 2

461 ng/mL DAPI using 30 min incubations at 30°C. Cell samples were finally resuspended in 100 μ L
462 of 2 \times SSC buffer. Imaging was performed on an Olympus IX71 inverted microscope with
463 excitation provided by a filtered mercury arc lamp. Data processing was performed with custom
464 Matlab code as previously described [45], with slight modifications for bacterial cell
465 identification using images collected with the DAPI filter.

466 ***Microfluidic chip fabrication and continuous cell culture.*** The microfluidic device consisted of
467 33 mixing channels, ascending from 3 to 8 per row, merging into a single cell growth chamber
468 (3.4 \times 1mm/length \times width). (Suppl Fig. 2A) Each cell growth chamber contains an array of 18
469 (6 \times 3) cell trapping chambers (40 μ M diameter). The lithography photomask with the desired
470 chip layout was produced in-house by a 2 μ M Process Control Marker (PCM) with tolerance of
471 \pm 0.25 μ M following previously established protocols [19]. The polydimethylsiloxane (PDMS)
472 chip fabrication base and curing reagent were mixed at 10:1 ratio to a homogeneous solution and
473 degassed in a vacuum chamber for 15 min or until all bubbles disappeared. The degassed PDMS
474 mixture was poured over a SU-8 wafer with the designed microfluidic pattern, cured for 3h on a
475 80°C hot plate or overnight at room temperature. Before mounting the PDMS chip on a glass
476 slide, the inlet and outlet holes were punched out with a 40 μ m needle, cleaned with isopropanol,
477 and plasma treated at 50W for 300s. The PDMS and glass chip were aligned and bonded for 30
478 min at 60°C. Prior to inoculation of the microfluidic chip with bacterial or human cells, a 1 ml
479 syringe was attached to tubing and 70% ethanol was run through the microfluidic chip for 2h at
480 50 μ l/hour speed using a syringe pump, followed by sterile water wash for 1h, and infusion with
481 growth media for 2h at 50 μ l/hour. Bacterial cells were delivered into the growth chamber
482 through a seeding inlet with a 1 ml syringe using a syringe pump, and the fluid was run through
483 the chamber for 5 min. When the desired cell density was achieved, the cell seeding inlet was

484 clamped and the microfluidic chip mounted in a microscope incubator preheated to 37°C. The
485 microscope chamber was connected to 5% CO₂ through a gas flow regulation system when
486 human neutrophils were inoculated in the microfluidic device.

487 **Fluorescence Analysis.** Bacterial and human neutrophil cell death was observed with propidium
488 iodide, PI, added to the cell culture media at 1µg/ml and infused into the microfluidic growth
489 chamber after termination of antibiotic incubation. For imaging of neutrophil extracellular traps
490 (NETs), antibody against human citrullinated histone H3, H3CitArg2/8/17 (LS-C144555,
491 LifeSpan Biosciences, Seattle, WA) was linked to FITC via the Lightning-Link Fluorescent
492 Antibody Labeling kit (cat#707-0010, Novus Biologicals, Littleton, CO). FITC-labeled anti-
493 H3CitArg2/8/17 was added to LB media at 1:300 dilution and infused into the microfluidic chip
494 through the medium inlets for 18h at room temperature and 2µl/hour flow speed. LB media alone
495 was supplied for another 18h to wash the unbound antibody, and florescent images were taken at
496 520/610 ex/em and 488/520 ex/em with a Zeiss Axio Observer Z1 microscope to capture nucleic
497 acid and citrullinated histone H3 staining, respectively.

498 **Infection of mice and determination of tissue bacterial load.** The animal studies were carried
499 out in strict accordance with the recommendations in the Guide for the Care and Use of
500 Laboratory Animals of the National Institutes of Health and DoD Instruction 3216.01, dated
501 September 2010 and Army Regulation 40-22. The experimental protocol was approved by
502 IACUC (IACUC #0503014D) at University of Texas, Medical Branch, UTMB, and Animal Care
503 and Use Review Office (ACURO) at US Army Medical Research and Materiel Command.

504 Female BALB/cJ mice, 6-week-old, obtained from Jackson Labs were used. Mice were allowed
505 to acclimate for 5 days prior to infection. Anesthetized BALB/c mice (n = 5 per treatment) were

506 inoculated intranasally (I.N.) with 2 LD₅₀ *B. pseudomallei* K96243, diluted in phosphate-
507 buffered saline (PBS) in a total volume of 50 µL (25 µL/ nare). Mice received daily
508 intraperitoneal injections of levofloxacin (25 mg/kg/day in PBS) starting at 24 h post-infection
509 and continuing for five days. Mice were monitored daily for weight changes and survival over a
510 period of 20-21 days. For CFU enumeration, animals were euthanized and their lungs, livers and
511 spleens collected for CFU enumeration and homogenized using Covidien Precision tissue
512 grinders (Fisher Scientific). Tissue homogenates were serially diluted in PBS, plated, and
513 incubated for 48 h at 37°C. Colonies were counted and normalized to organ weight (g).

514 **Statistics.** For the *in vitro* data of antibiotic effect on bacterial survival, we applied paired
515 Student's t test. Survival curves were analyzed by using the Kaplan-Meier method. A significant
516 difference ($p \leq 0.05$) in survival curves was ascertained via a log-rank test. CFU enumeration
517 significance was determined using T-test with a Mann-Whitney correction. We considered a P
518 value below 0.05 as significant.

519

520

521 **Acknowledgements**

522

523 This work was funded by a grant to EHG from the Defense Threat Reduction Agency (DTRA) of
524 the Department of Defense (DoD). The funders had no role in study design, data collection and
525 interpretation, or the decision to submit the work for publication. This work was performed, in
526 part, at the Center for Integrated Nanotechnologies, an Office of Science User Facility operated
527 for the U.S. Department of Energy (DOE) Office of Science.

528

529 **References**

- 530 1. **Spoering AL and Lewis K.** 2001. Biofilms and Planktonic Cells of *Pseudomonas*
531 *aeruginosa* have similar resistance to killing by antimicrobials. *Journal of Bacteriology*
532 183:6746.
- 533 2. **Lewis K.** 2006. Persister cells, dormancy and infectious disease. *Nature Reviews*
534 *Microbiology* 5:48.
- 535 3. **Smith PA and Romesberg FE.** 2007. Combating bacteria and drug resistance by
536 inhibiting mechanisms of persistence and adaptation. *Nature Chemical Biology* 3:549.
- 537 4. **Kussell E, Kishony R, Balaban NQ and Leibler S.** 2005. Bacterial Persistence: A
538 model of survival in changing environments. *Genetics* 169:1807.
- 539 5. **Keren I, Shah D, Spoering A, Kaldalu N, and Lewis K.** 2004. Specialized persister
540 cells and the mechanism of multidrug tolerance in *Escherichia coli*. *Journal of*
541 *Bacteriology* 18:8172.
- 542 6. **Germain E, Roghanian M, Gerdes K, and Maisonneuve E.** 2015. Stochastic induction
543 of persister cells by HipA through (p)ppGpp-mediated activation of mRNA
544 endonucleases. *Proceedings of the National Academy of Sciences of the United States of*
545 *America* 112:5171-6.
- 546 7. **Maisonneuve E, Shakespeare LJ, Jørgensen MG, and Gerdes K.** 2011. Bacterial
547 persistence by RNA endonucleases. *Proceedings of the National Academy of Sciences of*
548 *the United States of America* 108:13206-11.
- 549 8. **Harrison JJ, Wade WD, Akierman S, Vacchi-Suzzi C, Stremick CA, Turner RJ,**
550 **and Ceri, H.** 2009. The chromosomal toxin gene *yafQ* is a determinant of multidrug

- 551 tolerance for *Escherichia coli* growing in a biofilm. *Antimicrobial Agents and*
552 *Chemotherapy* **53**:2253-8.
- 553 9. **Allison KR.** 2011. Metabolite-enabled eradication of bacterial persisters by
554 aminoglycosides **473**:216-20.
- 555 10. **Conlon B, Nakayasu E, Fleck L, LaFleur M, Isabella V, Coleman K, Leonard SN,**
556 **Smith RD, Adkins JN and Lewis K.** 2013. Activated ClpP kills persisters and eradicates
557 a chronic biofilm infection. *Nature* **503**:365-70.
- 558 11. **Brötz-Oesterhelt H, Beyer D, Kroll H-P, Endermann R, Ladel C, Schroeder W,**
559 **Hinzen B, Raddatz S, Paulsen H, Henninger K, Bandow JE, Sahl HG, and**
560 **Labischinski H.** 2005. Dysregulation of bacterial proteolytic machinery by a new class
561 of antibiotics. *Nature Medicine* **11**:1082.
- 562 12. **Kirstein J, Hoffmann A, Lilie H, Schmidt R, Rübsamen-Waigmann H, Brötz-**
563 **Oesterhelt H, Mogk A, and Turgay K.** 2009. The antibiotic ADEP reprogrammes ClpP,
564 switching it from a regulated to an uncontrolled protease. *EMBO Molecular Medicine*.
565 **1**:37-49.
- 566 13. **Kyme P, Thoennissen NH, Tseng CW, Thoennissen GB, Wolf AJ, Shimada K, Krug**
567 **UO, Lee K, Muller-Tidow C, Berdel WE, Hardy WD, Gombart AF, Koeffler HP**
568 **and Liu GY.** 2012. C/EBP ϵ mediates nicotinamide-enhanced clearance of
569 *Staphylococcus aureus* in mice. *J. Clin. Invest.* **122**:3316-29.
- 570 14. **Bettenworth D, Nowacki, T. M., Ross, M., Kyme, P., Schwammbach, D., Kerstiens,**
571 **L., Thoennissen, G. B., Bokemeyer, C., Hengst, K., Berdel, W. E., Heidemann, J.**
572 **and Thoennissen, N. H.** 2014. Nicotinamide treatment ameliorates the course of

- 573 experimental colitis mediated by enhanced neutrophil-specific antibacterial clearance.
574 Mol Nutr Food Res. **58**:1474–90.
- 575 15. **Germain E, Roghanian M, Gerdes K, Maisonneuve E.** 2015. Stochastic induction of
576 persister cells by HipA through (p)ppGpp-mediated activation of mRNA endonucleases.
577 Proceedings of the National Academy of Sciences of the United States of America
578 **112**:5171-6.
- 579 16. **Li M, Long Y, Liu Y, Liu Y, Chen R, Shi J, Zhang L, Jin Y, Yang L, Bai F, Jin S,**
580 **Cheng Z, and Wu W.** 2016. HigB of *Pseudomonas aeruginosa* enhances killing of
581 phagocytes by up-regulating the Type III Secretion System in ciprofloxacin induced
582 persister cells. *Frontiers in Cellular and Infection Microbiology* **6**:125.
- 583 17. **Hemsley CM, Luo JX, Andreae CA, Butler CS, Soyer OS, Titball RW.** 2014.
584 Bacterial drug tolerance under clinical conditions is governed by anaerobic adaptation but
585 not anaerobic respiration. *Antimicrobial Agents and Chemotherapy*. **58**:5775-83.
- 586 18. **Chierakul W, Anunnatsiri, S. Short, J., Maharjan, B., Mootsikapun, P., Simpson,**
587 **A., Limmathurotsakul, D., Cheng, A., Stepniewska, K., Newton, P., Chaowagul, W.,**
588 **White, N., Peacock, S., Day, N., Chetchotisakd, P.** 2005. Two randomized controlled
589 trials of ceftazidime alone versus ceftazidime in combination with trimethoprim-
590 sulfamethoxazole for the treatment of severe melioidosis. *Clinical Infectious Diseases*
591 **41**:1105-13.
- 592 19. **Gruenberger A, Probst C, Heyer A, Wiechert W, Frunzke J, Kohlheyer D.** 2013.
593 Microfluidic picoliter bioreactor for microbial single-cell analysis: fabrication, system
594 setup, and operation. *Journal of Visualized Experiments:JoVE*. **82**:50560.

- 595 20. **Potrykus K and Cashel M.** (p)ppGpp: Still magical? 2008. Annual Review of
596 Microbiology **62**:35-51.
- 597 21. **Kaspar J, Kim JN, Ahn SJ, Burne RA.** 2016. An essential role for (p)ppGpp in the
598 integration of stress tolerance, peptide signaling, and competence development in
599 *Streptococcus mutans*. Frontiers in Microbiology. **7**.
- 600 22. **Kaplan MJ and Radic M.** 2012. Neutrophil extracellular traps (NETs): Double-edged
601 swords of innate immunity J. Immunol. **189**:2689-95.
- 602 23. **Mauracher LM, Posch F, Martinod K, Grilz E, Däullary T, Hell L, Brostjan C,**
603 **Zielinski C, Ay C, Wagner DD, Pabinger I, and Thaler J.** 2018. Citrullinated histone
604 H3, a biomarker of neutrophil extracellular trap formation, predicts the risk of venous
605 thromboembolism in cancer patients. Journal of Thrombosis and Haemostasis **16**:508-18.
- 606 24. **Schweizer HP.** 2012. Mechanisms of antibiotic resistance in *Burkholderia pseudomallei*:
607 implications for treatment of melioidosis. Future Microbiol. **7**:1389-99.
- 608 25. **Rhodes KA and Schweizer HP.** 2016. Antibiotic resistance in *Burkholderia* species.
609 Drug Resist Updat. **28**:82-90.
- 610 26. **Chow TK, Eu LC, Chin KF, Ong KC, Pailoor J, Vadivelu J, and Wong KT.** 2016.
611 Incidental splenic granuloma due to *Burkholderia pseudomallei*: A case of asymptomatic
612 latent melioidosis? The American Journal of Tropical Medicine and Hygiene **94**:522-4.
- 613 27. **Lobritz MA, Belenky P, Porter CBM, Gutierrez A, Yang JH, Schwarz EG, Dwyer**
614 **DJ, Khalil AS, Collins JJ.** 2015. Antibiotic efficacy is linked to bacterial cellular
615 respiration. Proceedings of the National Academy of Sciences of the United States of
616 America. **112**:8173-80.

- 617 28. **Lu S and Zgurskaya HI.** 2012. Role of ATP binding and hydrolysis in assembly of
618 MacAB-TolC macrolide transporter. *Molecular Microbiology* **86**:1132-43.
- 619 29. **Clark J F G, and Pinder S.** 1971. Inhibition of nuclear NAD nucleosidase and poly
620 ADP-ribose polymerase activity from rat liver by nicotinamide and 5'-methyl
621 nicotinamide. *Biochimica et Biophysica Acta.* **238**:82-5.
- 622 30. **Dalebroux ZD and Swanson MS.** 2012. ppGpp: magic beyond RNA polymerase.
623 *Nature Reviews Microbiology* **10**:203.
- 624 31. **Traxler MF, Summers SM, Nguyen H-T, Zacharia VM, Smith JT, Conway T.** 2008.
625 The global, ppGpp-mediated stringent response to amino acid starvation in *Escherichia*
626 *coli*. *Molecular Microbiology.* **68**:1128-48.
- 627 32. **Zhang T, Zhu J, Wei S, Luo Q, Li L, Li S, Tucker A, Shao H, Zhou R.** 2016. The
628 roles of RelA/(p)ppGpp in glucose-starvation induced adaptive response in the zoonotic
629 *Streptococcus suis*. *Scientific Reports* **6**:27169.
- 630 33. **Schulz JB, Matthews RT, Henshaw DR, Beal MF.** 1996. Neuroprotective strategies for
631 treatment of lesions produced by mitochondrial toxins: Implications for
632 neurodegenerative diseases. *Neuroscience* **71**:1043-8.
- 633 34. **Hathorn T, Snyder-Keller A, Messer A.** 2011. Nicotinamide improves motor deficits
634 and upregulates PGC-1 α and BDNF gene expression in a mouse model of Huntington's
635 disease. *Neurobiology of disease.* **41**:43-50.
- 636 35. **Ungerstedt JS, Blombäck M, Söderström T.** 2003. Nicotinamide is a potent
637 inhibitor of proinflammatory cytokines. *Clinical and Experimental Immunology.* **131**:48-
638 52.

- 639 36. **Stehr A, Ploner F, Tugtekin I, Matejovic M, Theisen M, Zülke C, Georgieff M,**
640 **Radermacher P, Jauch KW.** 2003. Effect of combining nicotinamide as a PARS-
641 inhibitor with selective iNOS blockade during porcine endotoxemia. *Intensive Care*
642 *Medicine* **29**:995-1002.
- 643 37. **Niren NM.** 2006. Pharmacologic doses of nicotinamide in the treatment of inflammatory
644 skin conditions: a review. *Cutis*. **77**:11-6.
- 645 38. **Smith IM and Burmeister LF.** 1977. Biochemically assisted antibiotic treatment of
646 lethal murine *Staphylococcus aureus* septic shock. *The American Journal of Clinical*
647 *Nutrition* **30**:1364-8.
- 648 39. **Brinkmann V, Reichard U, Goosmann C, Fauler B, Uhlemann Y, Weiss DS,**
649 **Weinrauch Y, and Zychlinsky A.** 2004. Neutrophil extracellular traps kill bacteria.
650 *Science*. **303**:1532.
- 651 40. **Clark SR, Ma AC, Tavener SA, McDonald B, Goodarzi Z, Kelly MM, Patel KD,**
652 **Chakrabarti S, McAvoy E, Sinclair GD, Keys EM, Allen-Vercoe E, Devinney R,**
653 **Doig, CJ, Green FH, Kubes P.** 2007. Platelet TLR4 activates neutrophil extracellular
654 traps to ensnare bacteria in septic blood. *Nature Medicine* **13**:463.
- 655 41. **Young RL, Malcolm KC, Kret JE, Caceres SM, Poch KR, Nichols DP, Taylor-**
656 **Cousar JL, Saavedra MT, Randell SH, Vasil ML, Burns JL, Moskowitz SM, and**
657 **Nick JA.** 2011. Neutrophil extracellular trap (NET)-mediated killing of *Pseudomonas*
658 *aeruginosa*: Evidence of acquired resistance within the CF airway, independent of CFTR.
659 *PLoS ONE* **6**:e23637.

- 660 42. **Dragovic J, Kim SH, Brown SL, Kim JH.** 1995. Nicotinamide pharmacokinetics in
661 patients. *Radiotherapy and Oncology: Journal of the European Society for Therapeutic*
662 *Radiology and Oncology.* **36:**225-8.
- 663 43. **Skokowa J, Lan D, Thakur BK, Wang F, Gupta K, Cario G, Brechlin AM,**
664 **Schambach A, Hinrichsen L, Meyer G, Gaestel M, Stanulia M, Tong Q, and Welte**
665 **K.** 2009. NAMPT is essential for the G-CSF-induced myeloid differentiation via a
666 NAD⁺-sirtuin-1-dependent pathway. *Nature Medicine.* **15:**151.
- 667 44. **Wilson WJ, Afzali MF, Cummings JE, Legare ME, Tjalkens RB, Allen CP, Slayden**
668 **RA, and Hanneman WH.** 2016. Immune modulation as an effective adjunct post-
669 exposure therapeutic for *B. pseudomallei*. *PLoS Neglected Tropical Diseases*
670 **10:**e0005065.
- 671 45. **Shepherd DP, Li N, Micheva-Viteva SN, Munsky B, Hong-Geller E, Werner JH.**
672 2013. Counting small RNA in pathogenic bacteria. *Analytical Chemistry.* **85:**4938-43.
- 673
- 674

675 **Figure Legends**

676

677 **Figure 1. NA enhances *B. thailandensis* sensitivity to antibiotics and stimulates persister**

678 **metabolism *in vitro*.** (A) *B. thailandensis* CDC2721122 cultures at exponential or stationary

679 phase were treated with bactericidal concentrations of Ofloxacin (100µg/ml), Ceftriaxone (150µg/ml) and

680 Tetracycline (250µg/ml) in the presence or absence of 1mM NA for 24h. Persister populations were

681 determined as percentage of the colony forming units (CFU/ml) surviving the antibiotic

682 treatment relative to the bacterial count prior to antibiotic exposure. Averages and std ± were

683 calculated from four independent experiments. (B) *B. thailandensis* cultures at stationary phase

684 were treated with Tetracycline (250µg/ml), Tetracycline (100µg/ml)+Ceftriaxone (50µg/ml), and Tetracycline

685 (100µg/ml)+Ceftriaxone (50µg/ml)+NA (1mM) for 24h. Persister populations were calculated as in (A)

686 and statistical analysis was performed on data obtained from three independent experiments. (C)

687 Bacterial cultures were grown in LB medium supplemented with 1mM NA, 10mM NA, or no

688 NA. The total ATP pool for *B. thailandensis* in the exponential and stationary phases was

689 measured as relative light units (RLU). A representative of five independent experiments is

690 shown and statistics were determined from three replicas from the same experiment. (D-E) *B.*

691 *thailandensis* cells were treated with 100µg/ml Ofloxacin, 200µg/ml Ofloxacin, and/or 1mM NA as

692 indicated at exponential phase. Samples were analyzed at 30 min intervals for ATP content (D)

693 and cellular density (E), by measuring luminescence and OD₆₀₀, respectively. A representative

694 of five independent experiments is shown. Averages and std ± were calculated from three

695 replicas per experimental condition.

696

697 **Figure 2. Antibiotic bactericidal effect against *B. thailandensis* persisters is dependent on**

698 **NA concentration. (A)** The microfluidic device was infused with 100 μ l *B. thailandensis* culture
699 (10^7 cells/ ml) in LB broth for 4h without flow to achieve universal distribution within the
700 growth chamber. Syringes containing LB broth supplemented with 0 and 100 μ M NA were
701 attached to the left and right inlet, respectively, and the flow speed was adjusted to 5 μ l per hour.
702 Bacterial density in the growth chamber was observed at 24h post infusion of NA with a Zeiss
703 Axio Observer Z1 microscope. Shown is a bright field image of bacterial density built from 6
704 image fields in the same row taken from left to right (low to high NA concentration) across the
705 width of the cell growth chamber. **(B)** Bright field image of bacterial growth in trapping
706 chambers of microfluidic device, built from 6 image fields in the same row taken from left to
707 right across the NA gradient. Syringes containing LB medium (left inlet) and LB supplemented
708 with 50 μ M NA (right inlet) were supplied into the growth chambers at 10 μ l/hr. *B. thailandensis*
709 cells (100 μ l, 10^7 cells/ml) were infused through the inoculation inlet and incubated for 24h in
710 the NA gradient prior to replacement with LB medium containing 50 μ g/ml Mpm for 48h,
711 followed by continuous flow with LB medium. **(C)** *B. thailandensis* growth in trapping chambers
712 after 4 days of antibiotic free media. PI (1 μ g/ml) was added to the LB medium, and cellular
713 viability was evaluated at 520/610 sex/em. Tile images were acquired covering the same row of
714 cell trapping chambers as in (B). A representative result of four independent experiments of
715 bright field (left panel) and fluorescence at 520/610 ex/em (right panel) is shown. **(D)** *B.*
716 *thailandensis* cultures (100 μ l, 10^7 cells/ml) were inoculated in microfluidic bioreactors infused
717 with LB media or LB supplemented with 4 μ M NA. Following 18h of bacterial growth in the
718 bioreactors, 50 μ g/ml Oflx was added to both experimental conditions. After 6 days of antibiotic
719 exposure, media was replaced with antibiotic-free LB at flow speed 5 μ l/hour, and the
720 microfluidic bioreactors were microscopically monitored for recovery of bacterial growth. PI

721 (1µg/ml) was added to the LB medium at day 3 of antibiotic withdrawal. Shown are microscopy
722 overlay images of bright field and 520/610 ex/em fluorescence at 5 days post antibiotic
723 withdrawal. A representative result of four independent experiments is shown.

724

725 **Figure 3. NA inhibits transcription of the stringent response regulator RelA in *B.***
726 ***thailandensis*.** (A) Total RNA was isolated from exponential and stationary phase *B.*
727 *thailandensis* grown in LB supplemented with 1mM NA and subjected to one step RNA-to-Ct
728 value RT-qPCR analysis. *relA* RNA levels were calculated relative to gene expression levels in
729 exponential cells grown in LB with no NA supplementation. Shown are *relA* RNA ratios
730 normalized to the chaperone *dnaJ* as a sample loading control. Averages and sdev± were
731 calculated from 3 independent experiments. (B) RNA FISH histograms of *relA* fluorescent
732 intensity distribution in single cells from exponential and stationary cultures of *B. thailandensis*
733 in LB medium or LB supplemented with 1mM NA. Cells were fixed and hybridized to 1µM
734 fluorescently labeled probes against *relA* transcripts. A representative from four independent
735 experiments is shown.

736

737 **Figure 4. NA stimulates the release of neutrophil extracellular traps (NETs).** Microfluidic
738 bioreactors were infused with FITC-labeled primary antibodies specific to human citrullinated
739 histone H3 and 1 µg/ml PI 20h after co-culture of *B. thailandensis* cells with human neutrophils.
740 Shown are overlay fluorescent microscope images of *B. thailandensis*/neutrophil co-culture (top)
741 not treated with NA and (bottom) neutrophils pre-treated with 100µM NA prior to bacterial
742 infection and subsequently incubated in media containing 25µM NA. Cells were imaged at
743 488/540ex/em and 520/610 ex/em, respectively. Histone H3 is seen as green or yellow overlay

744 staining.

745

746 **Figure 5. Immunoprophylaxis with high dose of NA resulted in increased host mortality**
747 **and enhanced persistence of *B. pseudomallei* in target organs.** (A) A high dose of NA

748 increased the survival rates of *B. pseudomallei* K96243 in response to levofloxacin. Stationary
749 phase bacterial cultures of *B. pseudomallei* K96243 were diluted 2-fold with fresh LB containing
750 100xMIC levofloxacin, or a combination of antibiotic and NA at the indicated concentrations.

751 Bacterial cultures were incubated for 24h at 37°C with no aeration. Percentage survival was
752 determined as CFU/ml of antibiotic treated cells versus the bacterial counts prior to antibiotic

753 treatment. The statistics were obtained from 6 experimental replicas. Mice (n=5) were pretreated
754 with NA or PBS 2 days prior to infection with 2 LD₅₀ of *B. pseudomallei* K96243. After

755 infection mice received either PBS, continued NA treatment, levofloxacin, or levofloxacin in
756 combination with NA starting 24-hours following infection and lasting 5 days. Through the

757 course of infection, weight (B) and survival (C) were monitored. At 21-days post-infection the
758 liver (D), spleen (E), and lungs (F) were collected for CFU enumeration of residual bacteria.

759 Gross histopathology differences between mice treated with levofloxacin (left) or levofloxacin in
760 combination with NA (right) are displayed in (G). Survival curves were analyzed by log-rank

761 test and asterisks indicate statistically significant difference between treatments (P<0.05, *).

762

763 **Fig. S1. ATP pool increase in antibiotic-treated *B. thailandensis*.** *B. thailandensis* cells were

764 treated at the exponential phase with 100µg/ml Mpm, 1mM NA, or a combination of antibiotic
765 with NA. Samples were analyzed at 30 min intervals for cellular density by measuring OD₆₀₀

766 (A) and ATP content (B) applying BacTiter Glo reagent (Promega). RLU, relative light units. A

767 representative of three independent experiments is shown.

768

769 **Fig. S2. Use of microfluidic bioreactors to study the effect of NA on bacterial sensitivity to**

770 **antibiotic treatment. (A) Design of the microfluidic chip.** Left panel shows layout of the

771 whole microfluidic chip with two inlets for media infusion (a1), a gradient generator with mixing

772 chambers (a2), cell infusion inlet (a3) and cell growth chamber containing array of cell trapping

773 chambers (a4). The right panel shows the design of cell trapping chambers with inner diameter of

774 40 μ m and 10 μ m depth. **(B) Metabolite concentrations in the microfluidic bioreactor was**

775 **estimated relative to the concentration gradient of a colorimetric dye.** A syringe pump was

776 used to inject two solute streams into the gradient generator. LB and LB media infused with

777 green dye were supplied through the media inlets (a1) feeding into channel 1 and channel 8,

778 respectively, at speed 10 μ l/hour. Microscopic images were obtained from channel 1 through 8 in

779 the cell growth chamber (a3). Image pixel number corresponding to color intensity in each

780 channel was used to calculate the fraction of dye input concentration via Igor software application.

781 A representative of 3 independent experiments is shown. Linear correlation between the dye

782 concentration and optical density could be achieved three channels removed from the dye input

783 channel 8. For the channels 1-6 the fraction of input concentration was used to estimate the

784 approximate drug or metabolite concentration.

785

786 **Table 1.** Effect of antibiotic type, dose and NA supplementation on the recovery time of *B.*
 787 *thailandensis* persister populations.

788

Experimental condition	Recovery in LB (Days)	789
Mpm (50 µg/ml)	4	
Tmp (400 µg/ml)	4	790
Oflx (50 µg/ml)	5	
Oflx (100 µg/ml)	10	791
Mpm (50 µg/ml) and 4 µM NA in medium	5	
Mpm (50 µg/ml), Neutrophils	7	
Mpm (50 µg/ml), Neutrophils, 4 µM NA in medium	7	
Mpm (50 µg/ml), Neutrophils, 25 µM NA in medium	12	
Mpm (50 µg/ml), Neutrophils pretreated w/ 50 µM NA, 4 µM NA in medium	15 days	
All experiments were independently repeated at least three times.		

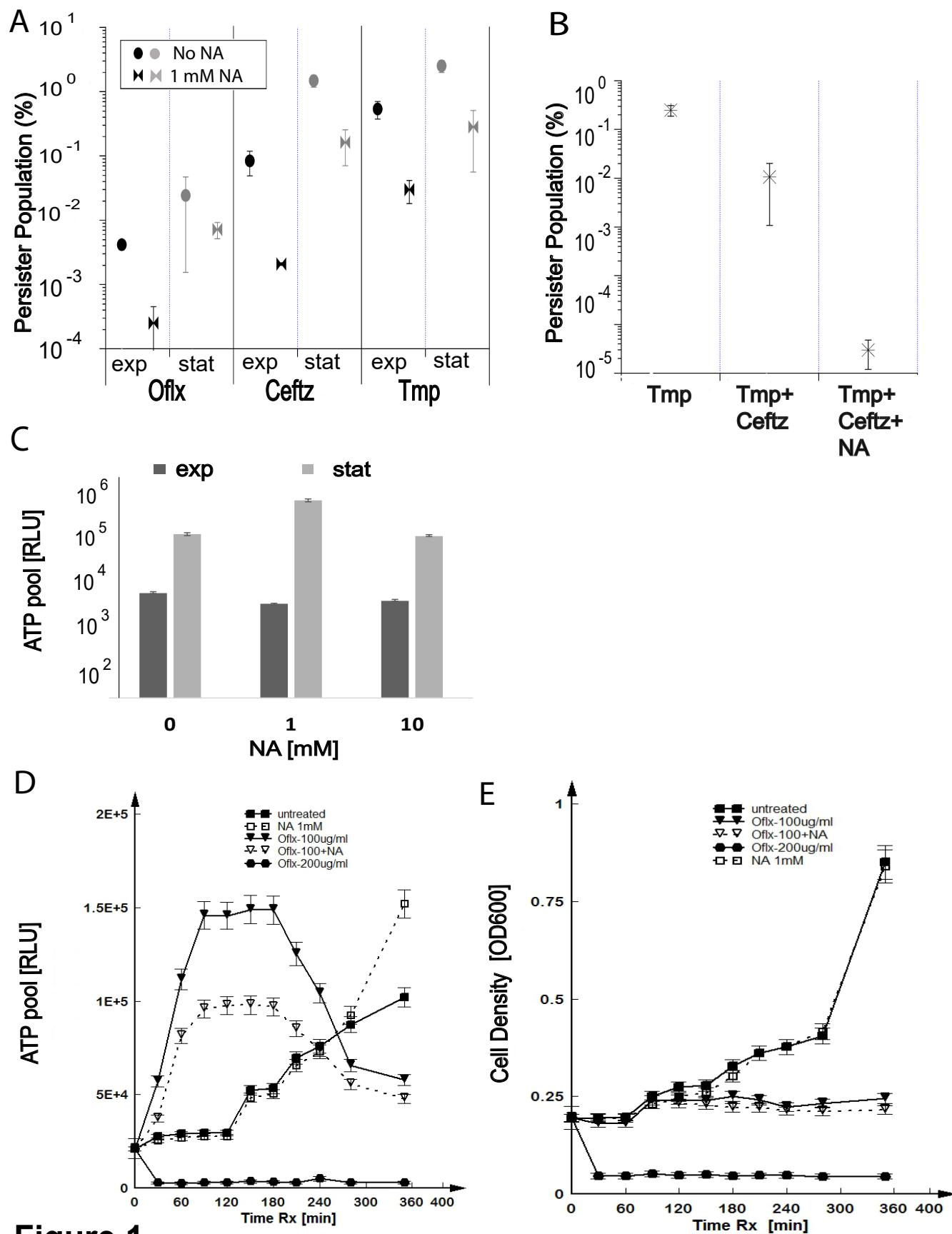
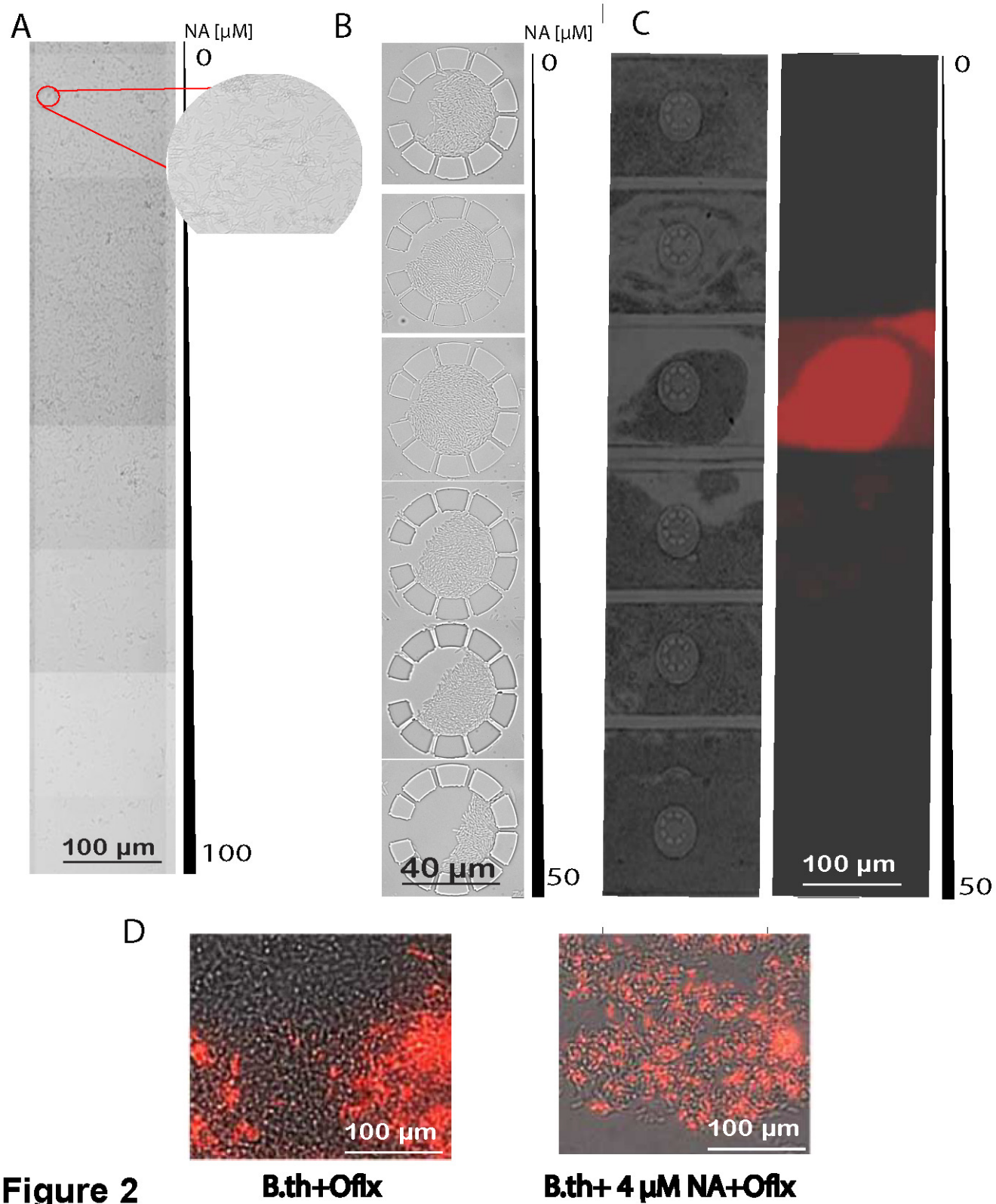


Figure 1



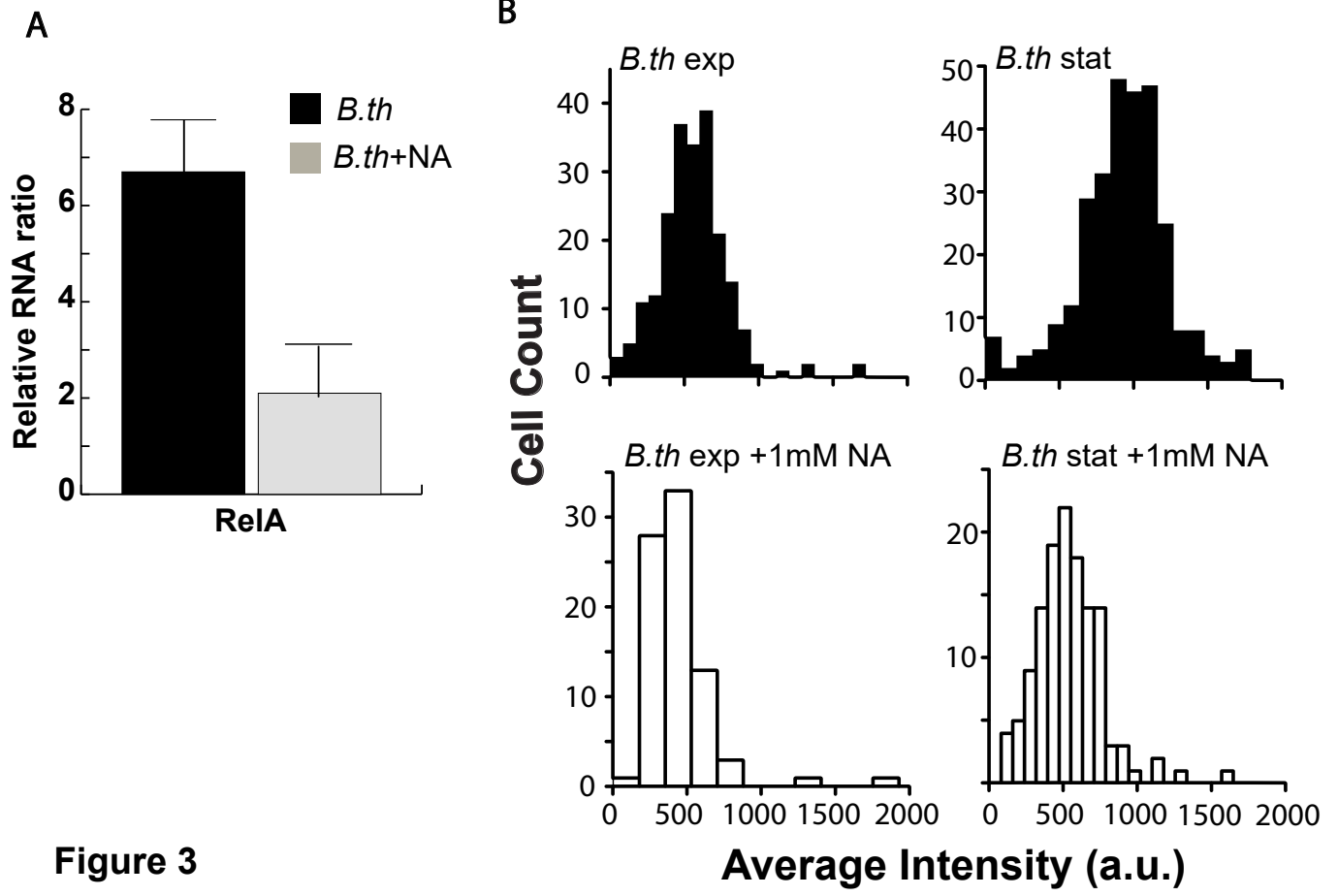


Figure 3

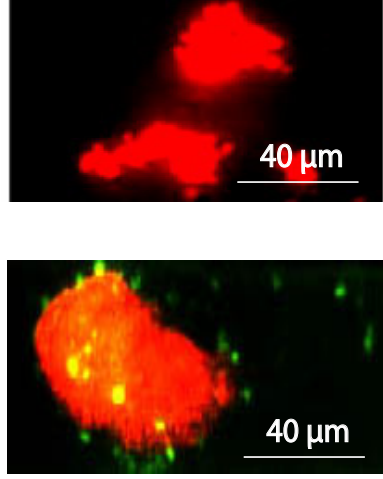


Figure 4

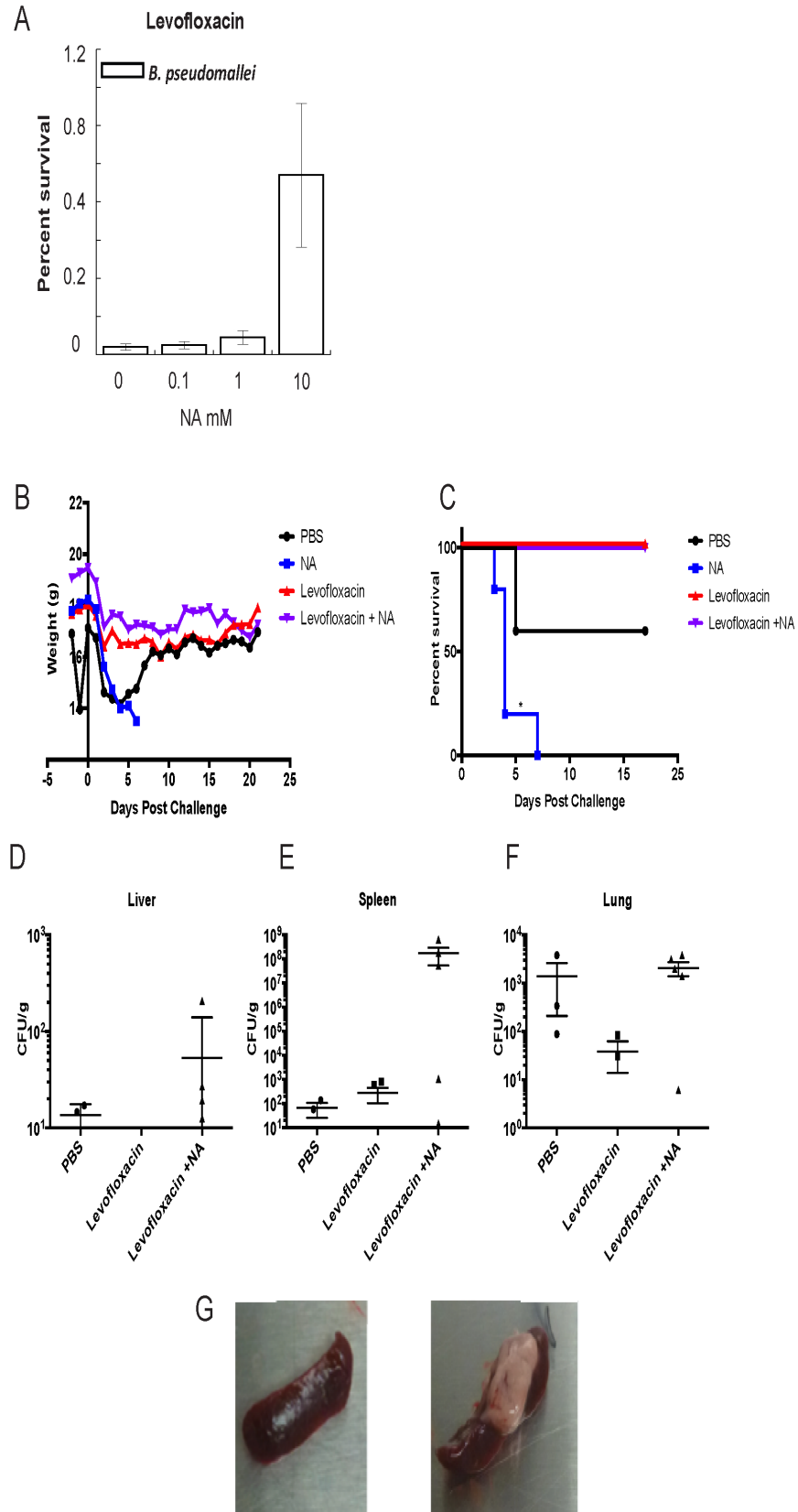


Figure 5